International Journal of Environmental Sciences
ISSN: 2229-7359
Vol. 11 No. 17s, 2025
https://theaspd.com/index.php

Power Quality Enhancement in Grid-Connected Solar PV via Shunt Active Filters and Optimized MPPT Algorithms

Mohammed Zaid Khan[1], **Seema Agrawal**[2]

[1,2]Dept. of Electrical Engineering, [1,2]Rajasthan Technical University, Kota, India, [1]mzaidkhan.phd19@rtu.ac.in
[2]sagrawal@rtu.ac.in, [*]**Corresponding Author**: [1]mzaidkhan.phd19@rtu.ac.in

Abstract: *This research shows a novel shunt active power filter (SAPF) paired with an advanced pulse width modulation (PWM) controller designed to reduce source current distortion and enhance power quality. The PWM controller effectively cancels distortions and stabilizes output voltage by filtering notches at output, including and excluding LCL filter compensation. Simulations using Power Simulator (P-Sim) demonstrate that the SAPF combined with an LCL filter reduces total harmonic distortion (THD) in source current to about 2.71 percent, significantly lower than the THD in load currents. The LCL filter smooths and isolates high-frequency harmonics, though its size must balance harmonic reduction and transient protection. The control method ensures that supply currents are sinusoidal, balanced, and maintain a unity power factor, compensating for unbalanced nonlinear loads and reactive power. The current controller responds quickly without causing transients, keeping the supply current below the load current, and efficiently lowering the THD. Additionally, the system integrates an optimum power point (MPPT) controller tracking based on the perturbation and observation (P&O) technique for grid-connected inverters, improving the grid-renewable energy interfacing. In general, the combination of innovative SAPF, PWM control, LCL filtering, and notch filter compensation provides an effective harmonic mitigation strategy and consequently a more optimized and reliable solar photovoltaic system with enhanced power quality.*

Keywords*: Pulse Width Modulator (PWM), Maximum Power Point Tracking (MPPT), Active Power Filter (APF), Voltage Source Inverter(s) (VSI), Photo voltaic (PV) generation*

1. INTRODUCTION

This research focuses on novelty in improving power quality in solar photovoltaic systems by developing a novel shunt active] filter (SAPF) and an advanced pulse width modulation (PWM) controller. The system uses a bridge source DC to AC converter with insulated gate bipolar transistors (IGBTs) to change DC into high-frequency AC, simulating the sinusoidal voltage of the utility grid. The prime challenge pois to eliminate source current distortions and regulate output voltage. Performance is evaluated by analyzing source, filter, and load currents using the new PWM controller, both with and without LCL filter compensation. The LCL filter helps in filtering notches at the load terminals, enhancing overall system stability and power quality. Therefore, a significant rejection in the source current distortion which proves the highly efficient designed novel PWM. The novel PWM controller for novel shunt active power filter nullify source current distortion. The innovative PWM controller for the new shunt active power filter (SAPF) effectively eliminates source current distortion. This SAPF and PWM controller work together to interface the grid with a solar photovoltaic (PV) array. A solar PV module converts sunlight into electrical energy through photovoltaic cells, providing clean and renewable power. The SAPF serves as a power conditioning device designed to enhance electrical power quality and system efficiency. It addresses common power quality challenges such as harmonic distortion, reactive power issues, and load imbalances, ensuring smoother and more reliable power delivery. Therefore, modulated signals are feeding in terms of voltage magnitude bringing via voltage sensors to Perturbed and Observed Algorithm. Since the algorithm acknowledges the novel pulse width modulated (PWM) controller, resultantly little change in the magnitude of voltage and current alters the magnitude of power. So, the comparative value of change in power switching over to optimize the value of power depending upon the magnitude of the change in the intensity of solar radiation and load variation. In a study from 2022 to 2024, a solar photo voltaic generation system utilizes a voltage source inverter and power electronic devices like insulated gate bipolar transistors (IGBTs) are used to convert direct current (DC) input into a high-frequency AC output, mimicking utility-supplied sinusoidal voltage [1-6]. A pulse width modulated controller, typically involving a microcontroller, regulates the on or off phases of the square wave signals for motor speed control. Active power filters enhance the power quality by reducing harmonics, and enhancing the power factor through compensatory currents, often by using PWM techniques [7-11]. Coupling inductors, which consist of coiled wires around

PWM techniques coupling inductors safeguard sensitive equipment from hazards, such as ground faults [17-18]. They regulate voltage fluctuations, reduce common-mode noise, and enhance safety [19]. Additionally, LCL compensation with Voltage Source Inverters improves the performance by addressing harmonic distortion and voltage stress in electrical systems [20]. The LCL filter network, comprising two inductors and a capacitor, mitigates harmonic distortion, improves the power factor [21-22].

2. Method

Case 1.

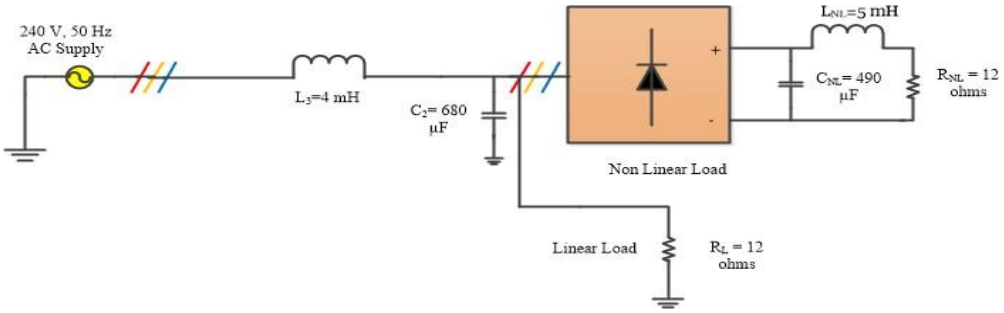

Fig. 1 Schematic of three phase supply with linear and non-linear load

As shown in Fig.1 above the schematic of three phase source with linear and non-linear load across its terminals with AC supply with a resistance and inductance in series. Since the specification of the system as shown in Table 1. Let us consider in case 1, the connection of non-linear load and linear load in parallel. As across the load terminals have capacitance. Furthermore, the characteristics of source and load current and its distortion including comparative characteristics of linear and non-linear load have obtained.

Table 1. Specification of the system

S.no.	Particulars	Quantity	Rating
	Source and Load Components		
1.	Source Voltage	3	230 volts, 50 Hz.
2.	Source inductances	1	L_1= 4 mH
3.	Non-linear load	1	L_{NL}= 5 mH, C_{NL}= 490 µF, R_{NL}= 12 ohms
4.	Linear Load	1	R_L= 12 ohms

Case 2: Let us consider case 2 and 3, as shown in Fig. 2, 3 and 4 common connection point (PCC) represents the point of supply required to synchronize the system. the value of the power, the multiplier feeds signal to the limiter. The limiter output obtains two comparative values of power decides the values of voltage either 0.5 volts or 0.6 volts depending upon the PV solar and AC grid interface using the novel PWM enhances the power quality as shown in Fig.5. This equation accounts for the photocurrent generated from sunlight and the effects of the diode characteristics and shunt resistance's effect on the output current; the output power (P_{out}) of the solar PV system is determined using equation (1):

$$P_{o=} V_{out} \text{ x } I_{out} \quad (1)$$

Therefore, the array obtains power P_{array}= 200 kW is the product of modules connected in series with parallel modules using the following equation (2):

$$P_{array}=N_s \cdot N_p \cdot P_m \quad (2)$$

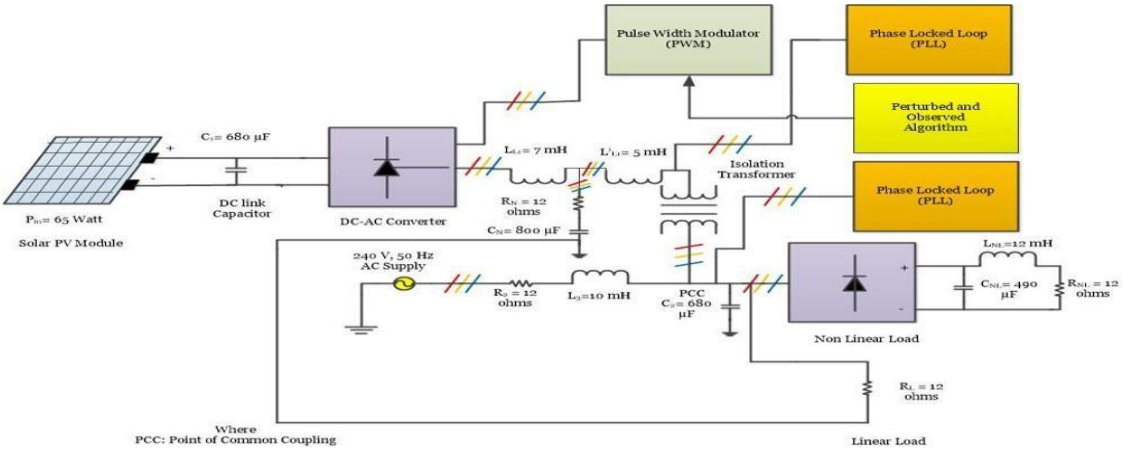

Fig. 2 Schematic of Solar PV Pulse Width Controlled Shunt Active Power Filter Using Perturbed and Observed MPPT Algorithm without LCL Compensation

P_{array}=10·66·300 W=199800 W around 200 kW, where: N_s = 10, is the series modules, N_p = 66, is the number of parallel modules, P_m is the power of each module (300 W) as shown in Table 2. Therefore, the IGBTs connected voltage and current sensors at the point of common coupling (PCC) via coupling inductor and isolation transformer, terminals, multiplies summation of dq parameters and pass-through low-pass filter featuring a gain value of 1 and a cut off frequency of 40 Hz. including damping ratio of 0.7. The Proportional Integral (PI) controller receives the signal and passes it with a gain of 0.2 along with a time constant of 0.00250. The output of the summation of the two signals from the PI controller fed a triangular wave with a peak-to-peak value of 360 volts and a frequency of 5 Hz. Therefore, the sine and cosine components give rise to the phase angle and frequency, respectively. Therefore, case 2 suggests an alternative measure to mitigate harmonics without compensation in the filter and source side by extracting output power and array power connects with the DC-AC converter. Since the isolation in the case 1 without filter and passive compensation at the load side. Therefore, the isolation transformer contributes a pivotal role. As the three-phase supply is connected with the Solar PV array interfacing with the supply grid makes a hybrid shunt active power filter with novel pulse width modulator. In addition to, the provision of LCL and notch filter compensation opens the way for mitigation of harmonics at the source and load side. Since the primary goal of this work is to reduce disturbances on both source and load sides. Therefore, the passive filter with notch filter further mitigates the supply harmonics.

Case 3: Consequently, power quality is enhanced of the hybrid system of Solar-grid integration. The main advantage of this schematic as shown in Fig. 3, is to simulate the perturbed and observed algorithm (PO). The algorithm step by step trace the peak power point and observe the next optimum point of maximum power to extract maximum power from the controller. The novel pulse width controller able to obtain proper duty cycle by triggering at the DC-AC converter as voltage source inverter (VSI) to trigger the signal on each and every gate of the grid. To align the phases of source current source resistances and inductance contributes a pivotal role, is further helpful in voltage, phase angle and phase sequence and enable phase Locked loop (PLL). Since phase-locked circuits are control to synchronize the phase of a signal with a reference signal, therefore with grid-connected inverters, the primary goal of this work is to reduce disturbances on both source and load sides. The use of PLLs in three-phase grid-connected inverters, including basic PLL operations, use of fault control, optimization of PLL parameters, impedance analysis, and development of new control strategies. Since Solar PV generation with SAPF is coupled to a triangular carrier in a phase-locked (PLL) context using pulse-width modulation (PWM) technology used to control the output voltage of the inverter. In a photovoltaic system, the inverter transforms the direct current from solar panels into alternating current suitable for grid connection. Pulse Width Modulation (PWM) is a method used to regulate the inverter's output voltage by comparing a high-frequency triangular carrier signal with a sinusoidal reference waveform, as illustrated in Fig. 6.

International Journal of Environmental Sciences
ISSN: 2229-7359
Vol. 11 No. 17s, 2025
https://theaspd.com/index.php

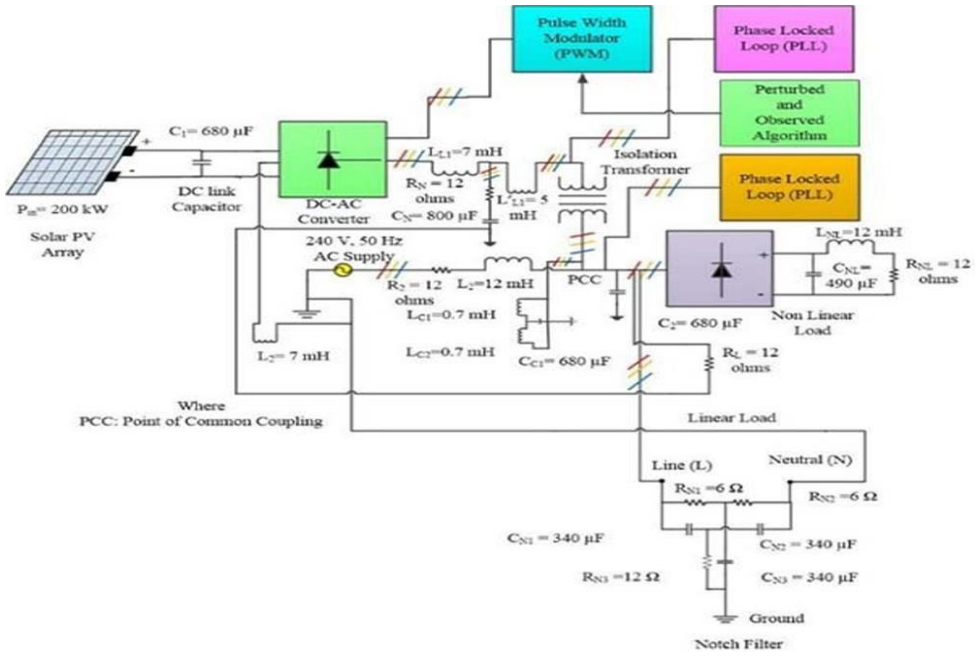

Fig.3 Schematic of Solar PV Novel Pulse Width Controlled Shunt Active Power Filter with MPPT Algorithm

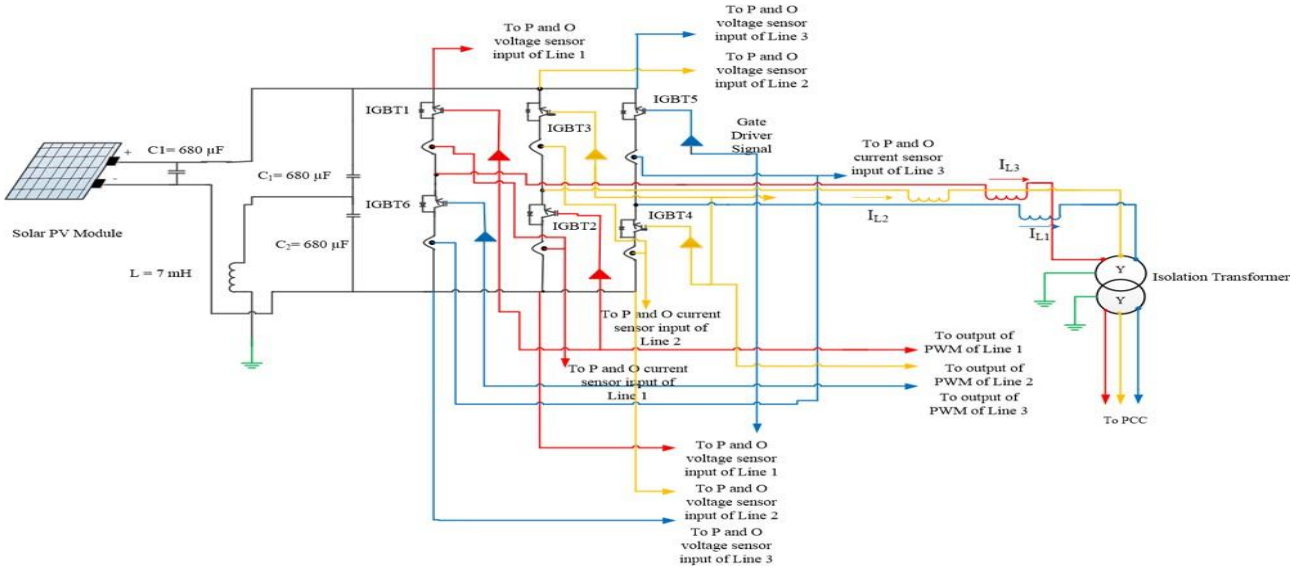

Fig.4 Schematic of bridge type DC-AC converter with connections

As illustrated in Fig.5, the transfer function with continuous-time for an integrator is given by as Equations (3) to (5):

$$I(s)=\frac{1}{s} \tag{3}$$

$$y[n]=y[n-1]+T.e[n] \tag{4}$$

where y[n] denotes the output of the integrator in the n-th sample. The continuous-time PI controller can be expressed in the Laplace domain as per equation (5):

$$C(s)= K_p + \frac{K_i}{s} \tag{5}$$

Table 2. Specification of the System

S.no.	Particulars	Quantity	Rating
		Solar Module	
1	PV solar Array	300 Watts/module x 666 modules	V_L = 132 volts, I_{sc}= 37 Amp. P_{in}= 200 kW
2	Capacitor across Solar Module	1	C_1= 680 µF
		Voltage Source Inverter	
3	IGBT	6	V_{sat}=0.6 volts, R_{Trans}= 0.028 volts, V_{diode}= 4 volts, R_{diode}=0.014 ohms
4	DC link capacitor	2	C_{link1}= C_{link2}= 680 µF
5	DC link Inductance	1	L_{link}= 7 mH
		Auxiliary Components	
6	Inductor	1	L_{L1}=7 mH, L'_{L1}= 5 mH, L_2= 7 mH
7	Neutral Earthing Resistor	3	R_{N1}=R_{N2}=R_{N3}=12 ohms
8	Neutral Earthing Capacitor	3	C_{N1}=C_{N2}=C_{N3}=800 µF
9	Isolation Transformer	1	N_1=N_2=1
		Pulse Width Modulator	
10	Pulse width modulator	1	V_{ref}=V_{dcin}-V_{dcout}=17.3 volts R= 40 ohms, f_{samp}= 1 kHz, V_{reftrt}= 0.5 volts, C_{par}= 450 µF, SR flip flop, Frequency= 50 kHz, Duty Cycle 50% %, R_{smit1}= 4 Ω, R_{smit2}= 3 Ω
11	Source impedance	1	0.5 Ω
12	Load Capacitance	1	680 µF
13	Phase locked loop	2	Triangular signal, V_{pp}=360 volts, f= 5 Hz., Duty Cycle= 12nd Order Low pass filter, Gain=1, f_{cutoff}= 40 Hz., Damping ratio =0.7 PI Controller, Gain=0.02, Time constant = 0.00250, Phase Delay = 120 º

Nomenclature: V_L= DC output voltage, I_{sc}= short circuit current in amperes, P_{in}= Input Power in kW, V_{sat}= Saturated voltage, R_{trans}= Transfer Resistance of IGBT, V_{diode}= diode like voltage drop, R_{diode}= diode like resistance, C_{link1}=C_{link2}= DC link capacitor, L_{link}= DC link inductance, R_{N1}=R_{N2}=R_{N3}= Neutral earthing resistors, C_{N1}=C_{N2}=C_{N3}= Neutral earthing capacitors, V_{ref}= Reference voltage in volts, V_{dcin}= DC input voltage in volts, f_{sample}= Sampling frequency in kHz, V_{reftrt}= Reference voltage in volts, C_{par}= Parasitic Capacitance in µF, V_{TD}= Threshold voltage in volts, R_D= Dynamic resistance in ohms, R_{smit1}=R_{smit2}= Smitt Triggering resistance in ohms, V_{pp}= peak to peak voltage in volts, and f_{cutoff}= cut off frequency in Hz

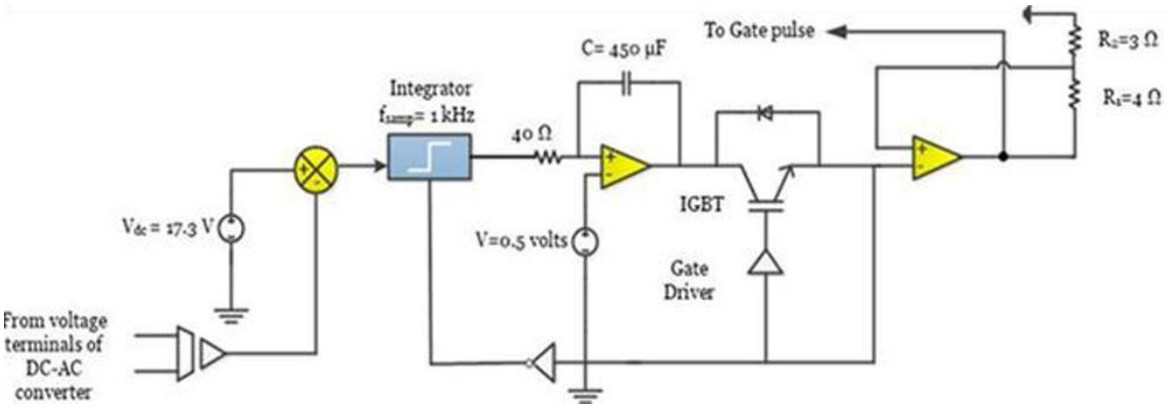

Fig. 5 Schematic of Novel Pulse Width Modulator

Since the control strategy in a solar PV-grid-tied system that use a low-pass filter to refine the signals. This approach helps maintain stability and optimize system operation in response to varying conditions. The control

International Journal of Environmental Sciences
ISSN: 2229-7359
Vol. 11 No. 17s, 2025
https://theaspd.com/index.php

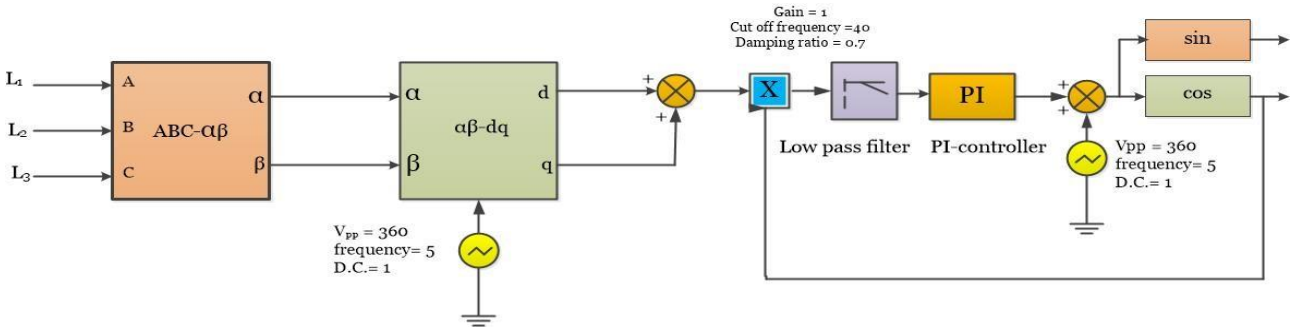

Fig. 6 Schematic of Phase Locked Loop

$$P_{pv}[n]= V_{pv}[n]\cdot I_{pv}[n] \quad (6)$$

equations are given by as shown in Fig.7 and (6)-(9*)*. where $P_{pv}[n]$ is the PV output power at the nth sample, $V_{pv}[n]$ is the PV voltage at the nth sample, $I_{pv}[n]$ is the PV current at the nth sample.

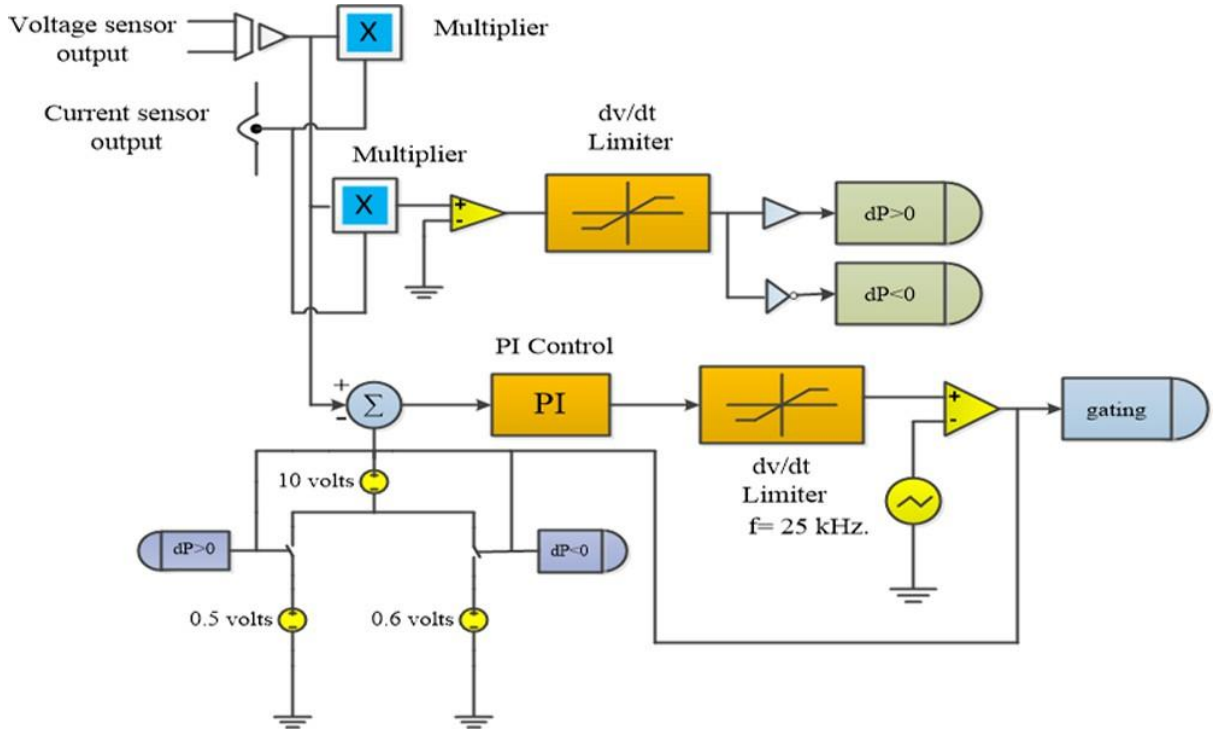

Fig. 7 Perturbed and Observed Control Algorithm for PWM based SAPF

$$\Delta P = P_{pv}[n]-P_{pv}[n-1] \quad (7)$$

$$\Delta V=V_{pv}[n]-P_{pv}[n-1] \quad (8)$$

$$V_{ref}[n]= \begin{cases} V_{pv}[n]+\Delta V_{step} \text{ if } \Delta P>0 \text{ and } \Delta V>0 \\ V_{pv}[n]-\Delta V_{step} \text{ if } \Delta P>0 \text{ and } \Delta V<0 \\ V_{pv}[n]-\Delta V_{step} \text{ if } \Delta P<0 \text{ and } \Delta V>0 \\ V_{pv}[n]+\Delta V_{step} \text{ if } \Delta P<0 \text{ and } \Delta V<0 \end{cases} \quad (9)$$

Since, Total harmonic distortion (THD) measures the level of distortion in a signal, especially in electrical and audio systems. The relation current THD is:

$$THD = \frac{\sqrt{\sum_{n=2}^{\infty} I_{nrms}^2}}{(I_{fundrms})} \quad (10)$$

$$\% THD = 100 \times \frac{\sqrt{I_2^2+I_3^2+I_4^2+\ldots+I_n^2}}{I_1} \quad (11)$$

3. RESULTS AND DISCUSSION

As per case 1 for no filter compensation subject to source and load current side exists, the supply magnitude of three phase voltages is 230 volts. At this voltage, the three phase average source side current is 20 to 40 amperes as shown in Fig.8,9.

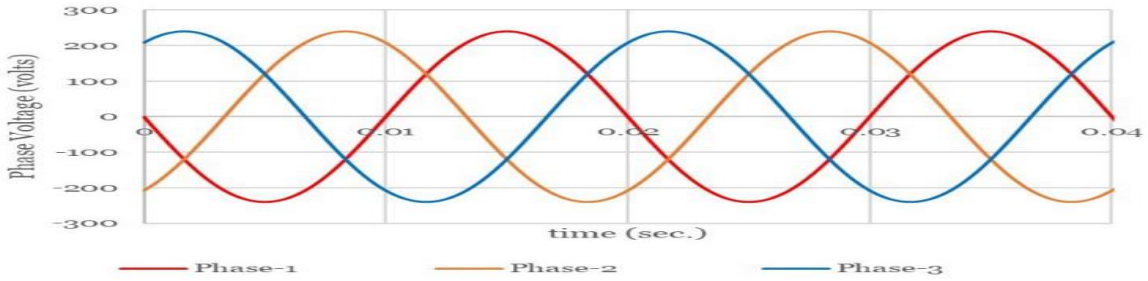

Fig.8 Supply three phase voltage

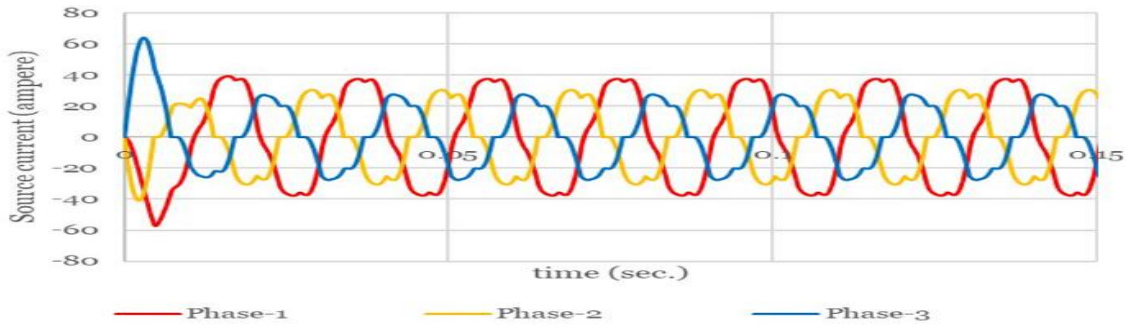

Fig.9 Source Side Current (ampere)

As harmonics maintain stable operation under varying load conditions as shown in Fig.10. The magnitude of linear and non-linear load currents shows average value around 20 amperes and 30 amperes respectively. Resultantly, filtration of output requires compensation devices to enhance the power quality. Also, the distortion in magnitude of source and load side current with frequency as shown in Fig.11. The source side and load side current distortion lie between around 23 % to 36 %. Therefore, it is obligatory to suppress the excessive loading and magnitude of load side current including mitigating the total harmonic distortion of source side current. As a result, the proposed further case studies discuss and make possible the mitigation of harmonics and suppression of excessive loading. The magnitude of source and load side response of % THD as shown in Table 3.

As illustrated in Fig. 12, the three-phase input voltage and current are 230 V AC. Also, source current is 18 amperes after tuning the parameters of the PWM controller as shown in Fig. 13. The PWM signals at the gate terminals of the IGBTs are valid with and without compensation, as shown in Fig. 14 (a), (b), and (c) for three phases L1, L2 and L3. Since the gate triggering is responsible forming current at the source, filter and load side as shown in Fig. 15. As a result, the total harmonic distortion of source and load current without LCL compensation as shown in Fig. 16 and 19. The value of source and load current in magnitude is about 15 ampere and the value of filter current in an average less than 5 ampere in magnitude. Since the load are of both types i.e. linear and non-linear. Resultantly, notches are obvious at the load side current. To nullify the notches LCL and notch filter are provided in another case study to reject load side disturbance. Therefore, comparative analysis of source, filter and load current without LCL compensation with THD of current as shown in Fig.15 and 16 respectively. Similarly

International Journal of Environmental Sciences
ISSN: 2229-7359
Vol. 11 No. 17s, 2025
https://theaspd.com/index.php

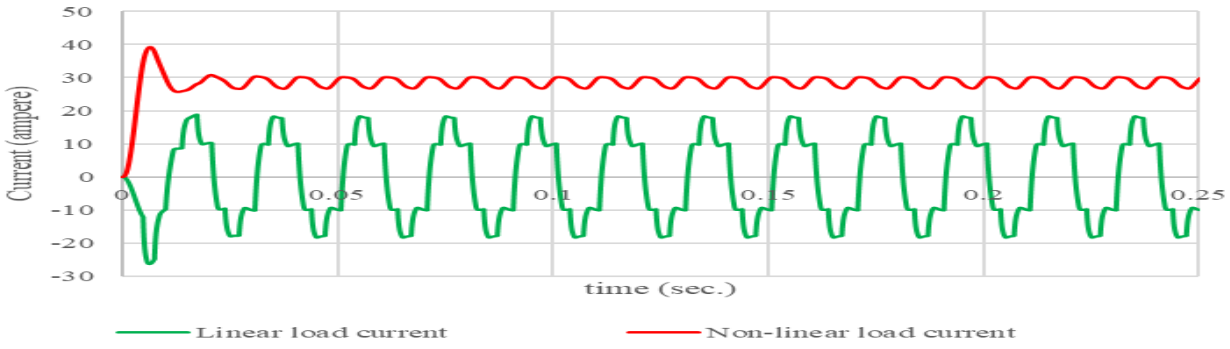

Fig.10 Linear and non-linear load current (ampere)

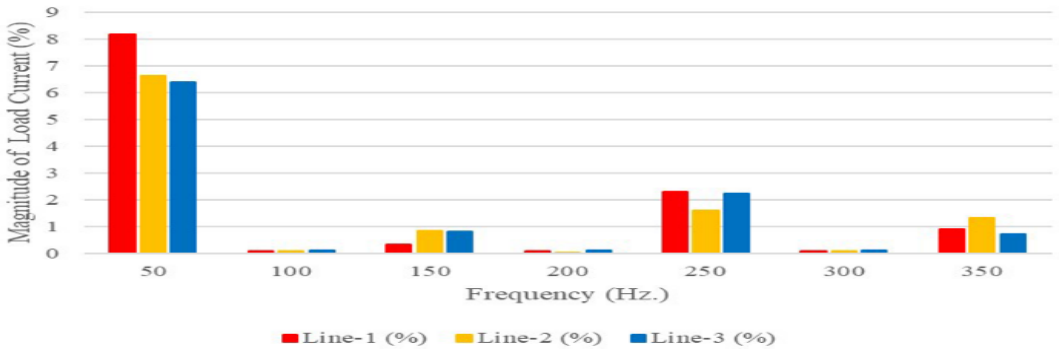

Fig.11 % THD of source current with linear and non-liner load for three phase AC supply with loads connected across its terminals

Table 3. Case 1: Comparison of % THD current of source and load with three phase AC supply and load

	Source side Current (%)		Load Side Current (%)
S.no.	Electrical Quantity	Percentage (%)	Percentage (%)
1.	% THD of I_{L1}	23.65	23.65
2.	% THD of I_{L2}	36.45	36.45
3.	% THD of I_{L3}	39.42	39.42

, Fig. 20 presents a comparative analysis of linear and nonlinear load currents. These load currents synchronize with the grid through the use of a phase-locked loop (PLL). The PLL ensures synchronization and balance by locking the three-phase grid voltages to the solar PV generation system, as depicted in Fig. 21 After obtaining the filter current, it is natural to obtain the filter and load voltages with THD of load current as shown in Fig. 17,18 and 19 respectively.]Ia]similar manner, the comparative analysis of linear and non-linear load current as shown in Fig.20. The resultant linear and non-linear load currents synchronize with the grid by enabling the phase locked loop (PLL). The phase locked loop (PLL) locks and balances by synchronizing three phase grid voltages to the solar PV generation system as shown in fig.21. Since the output source, filter and load current with Figure 22 illustrates the LCL and notch filter compensation. Filter and load currents remain below 5 amperes, while the source current is approximately 20 amperes. Additionally, the source current magnitude is nearly negligible in percentage terms, as shown in Figure 23. The filter and load voltages for all three phases are around 6 amperes, depicted in Figures 2, 24, and 25. Figure 26 presents the load current magnitude in percentage terms. The linear and non-linear load current with LCL

International Journal of Environmental Sciences
ISSN: 2229-7359
Vol. 11 No. 17s, 2025
https://theaspd.com/index.php

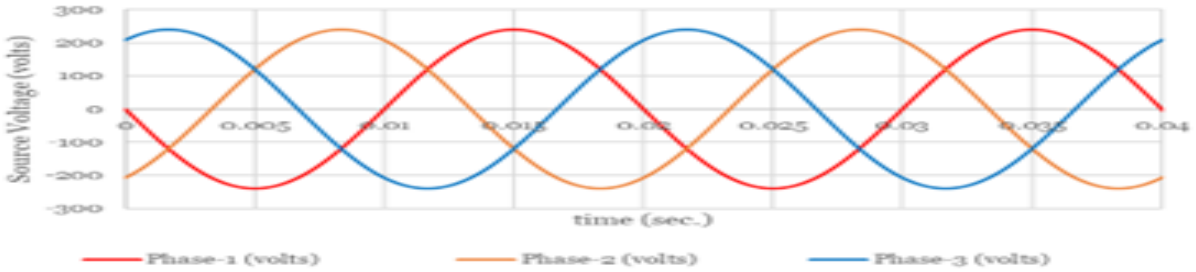

Fig. 12 Supply three phase voltage

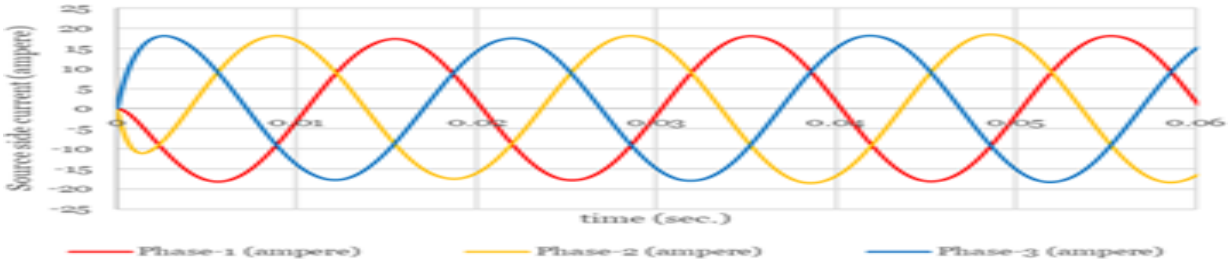

Fig. 13 Source Side Current (ampere)

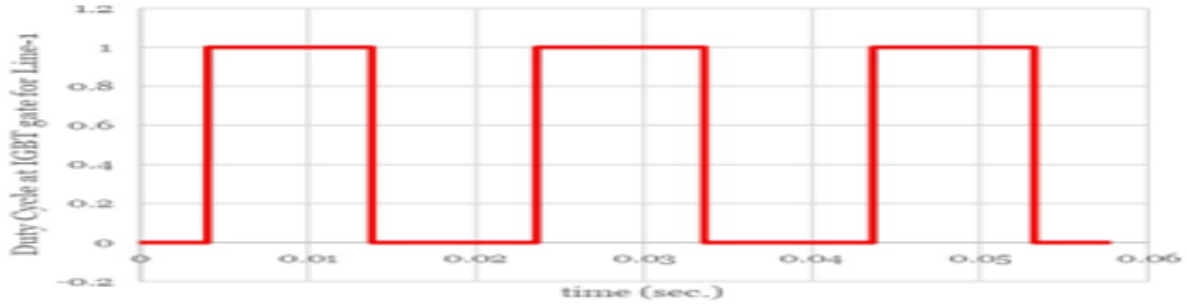

Fig.14 (a) Duty cycle at gate terminal for Phase L_1

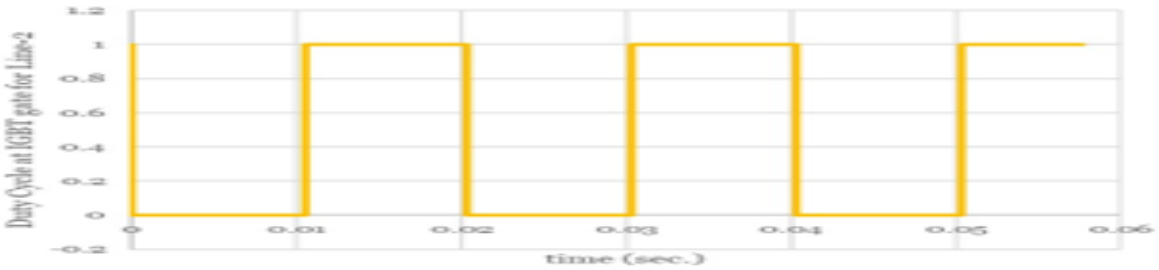

Fig.14 (b) Duty cycle at gate terminal for Phase L_2

compensation as shown in Fig. 27. The average value of both the current is 0.4 ampere. Since % THD comparison of source side and load side current without LCL compensation as shown in Table 4. The source side disturbance eliminates from 0.295 % but the load side current in percentage in terms of percentage is around 34 %. In a similar manner, the specification of LCL compensation with notch filter as shown in Table 5. Table 6 displays the percentage of total harmonic distortion (THD) for source and load currents with LCL compensation. The source current's % THD is nearly zero. and the load side is around 25 %. Resultantly, the PWM modulator without LCL compensation and with LCL compensation as shown in Table 7.

International Journal of Environmental Sciences
ISSN: 2229-7359
Vol. 11 No. 17s, 2025
https://theaspd.com/index.php

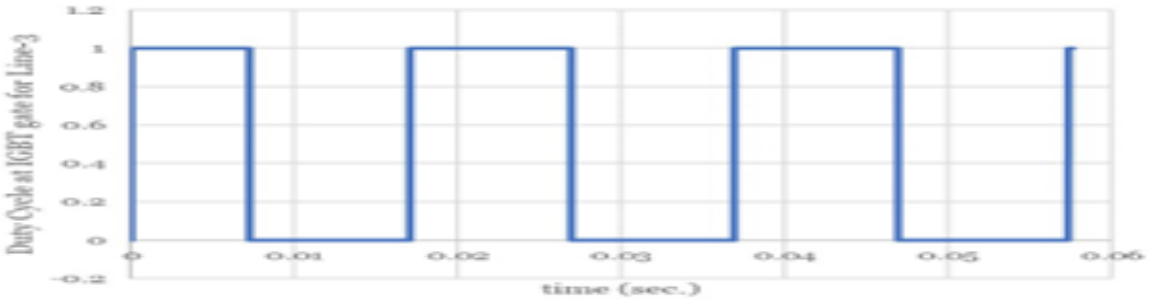

Fig.14 (c) Duty cycle at gate terminal for Phase L_3

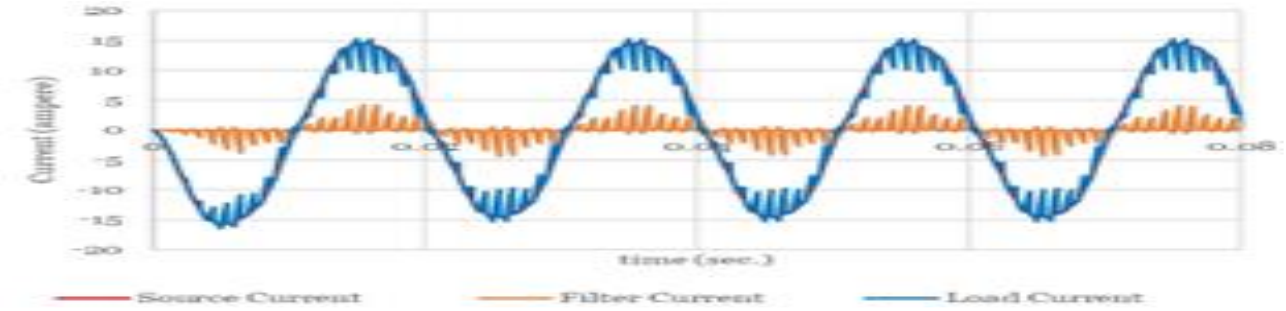

Fig. 15 Source, filter and load current versus time without LCL compensation and notch filter

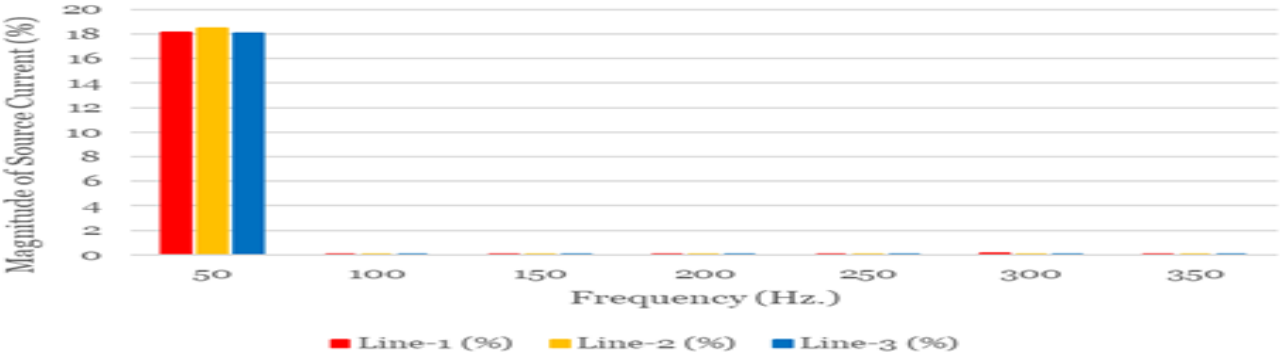

Fig.16 Magnitude of Source Current versus Frequency (%)

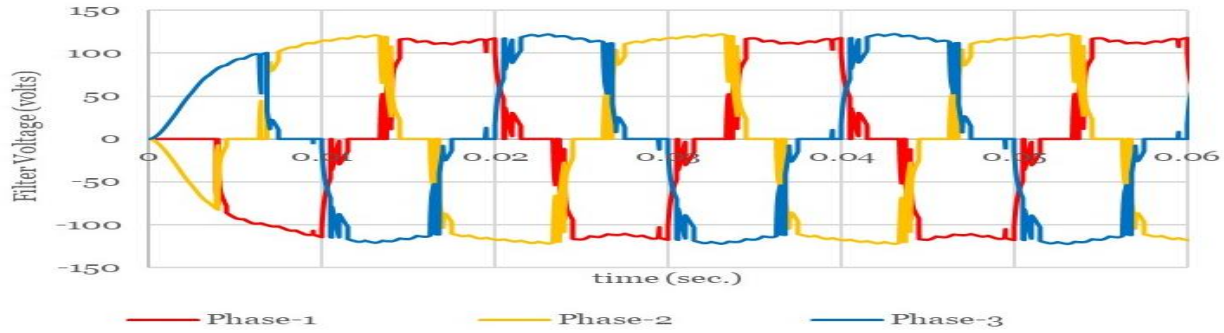

Fig.17 Filter Voltage (volts)

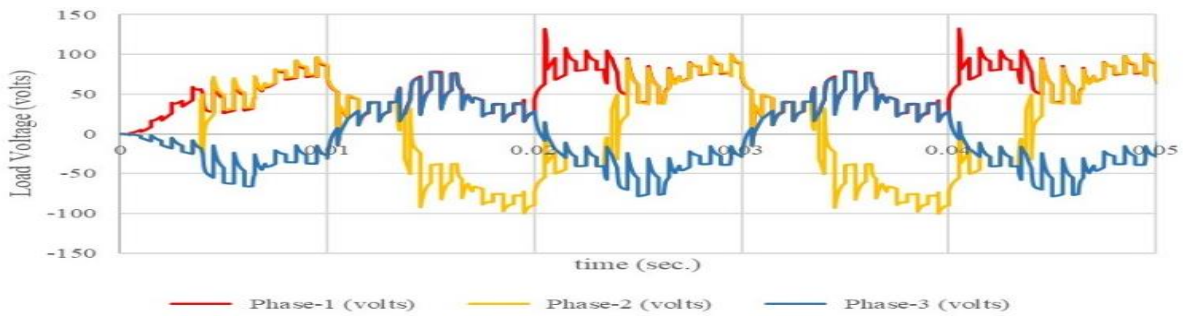

Fig. 18 Load Voltage (volts)

International Journal of Environmental Sciences
ISSN: 2229-7359
Vol. 11 No. 17s, 2025
https://theaspd.com/index.php

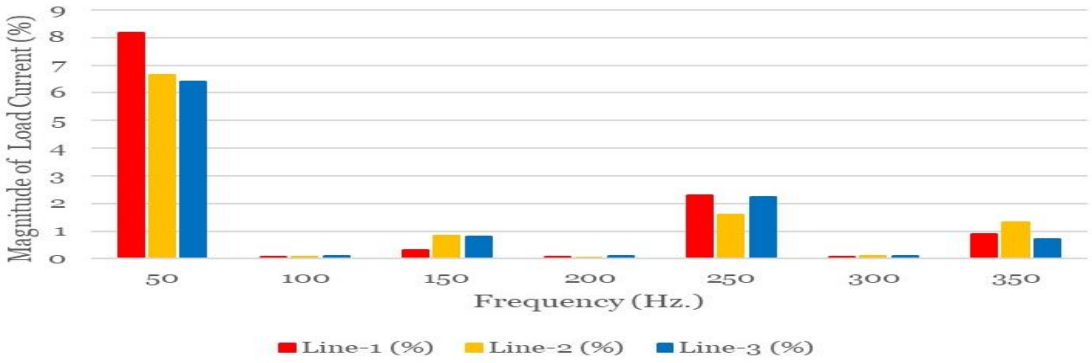

Fig. 19. Magnitude of Load Current (%) versus frequency (Hz.)

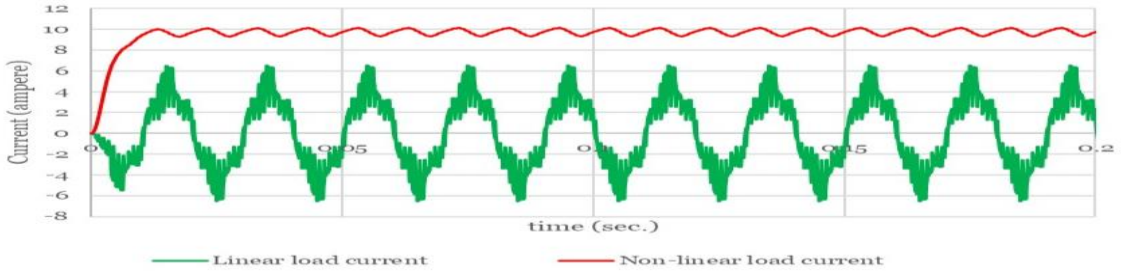

Fig. 20 Linear and non-linear load current (ampere)

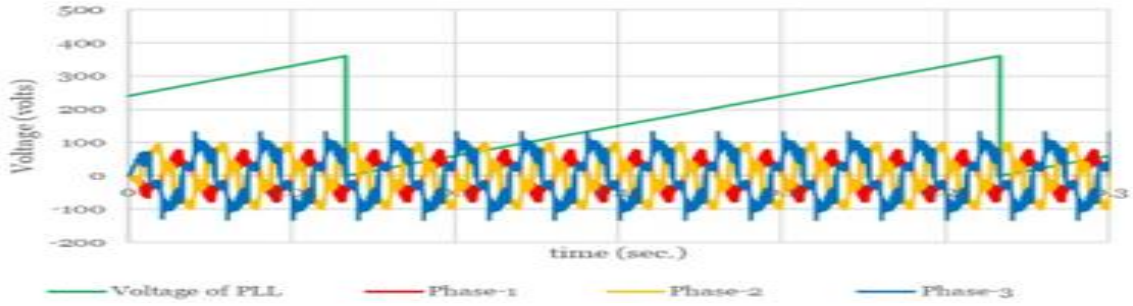

Fig. 21 Solar PV-Grid three phase voltage synchronization

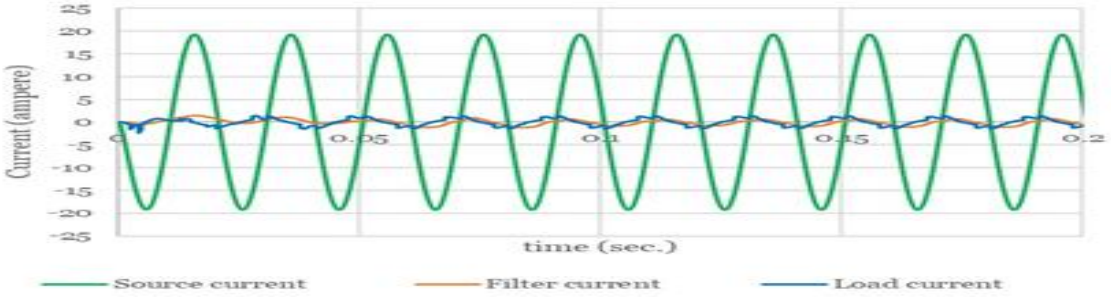

Fig. 22 Source, filter and load current versus time with LCL compensation and notch filter

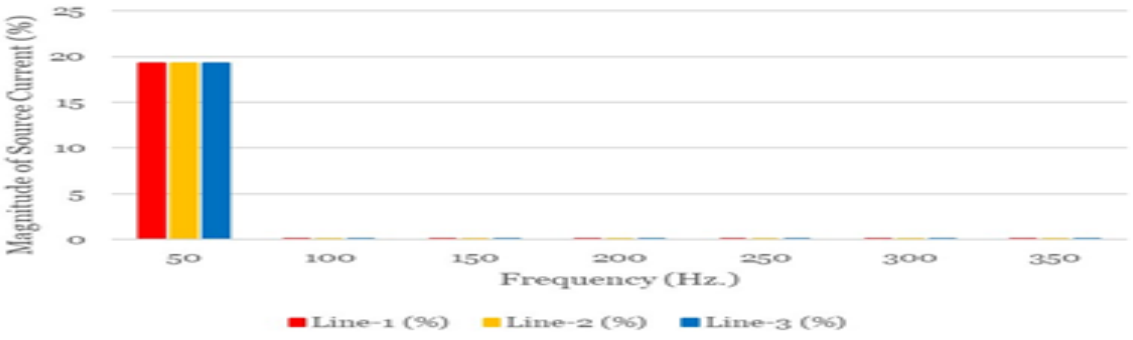

Fig.23 Magnitude of Source Current versus Frequency (%)

International Journal of Environmental Sciences
ISSN: 2229-7359
Vol. 11 No. 17s, 2025
https://theaspd.com/index.php

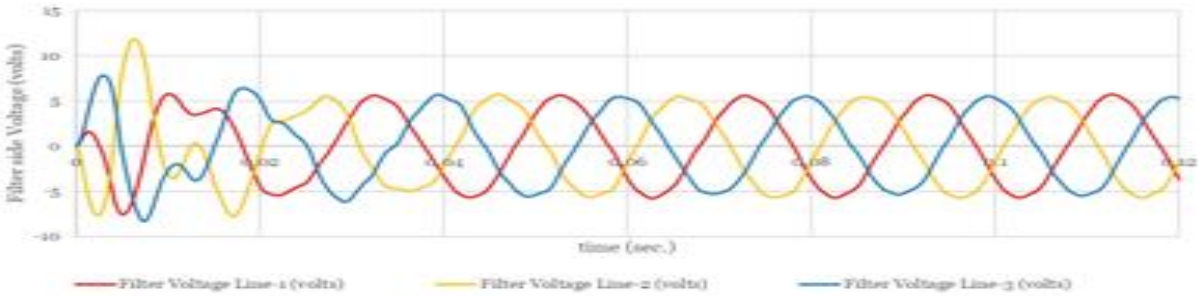

Fig. 24 Filter voltage (volts) with LCL compensation

Fig.25 Load Voltage (volts) with LCL compensation

As shown in Table 7, substantial reduction in the source side and load side current distortion PWM controller with LCL compensation as compared to without LCL compensation. Resultantly, the overall compensation requires simply source, filter and load side compensation. Therefore, the %THD comparison for without filter and LCL compensation. Secondly, as the term relates to %THD comparison of source, filter and load side current. Therefore, the power quality improves in case study 3 as compared to case 1 and 2.

Table 4. % THD Comparison of current of source and load without LCL compensation

		Source side Current (%)	Load Side Current (%)
S.no.	Electrical Quantity	Percentage (%)	Percentage (%)
1.	% THD of I_{L1}	0.601	20.35
2.	% THD of I_{L2}	0.451	30.65
3.	% THD of I_{L3}	0.295	33.96

Table 5. LCL and Notch Filter

S.no	PARTICULARS	QUANTITY	RATING
1.	LCL Filter	1	L_{C1}= L_{C2}=0.7 mH, C_{C1}=680 µF R_{N1}=R_{N2}=12Ω, R_{N3}= 6 Ω,
2.	Notch Filter	1	C_{N1}=C_{N2}=340 µF, C_{N3}= 680 µF

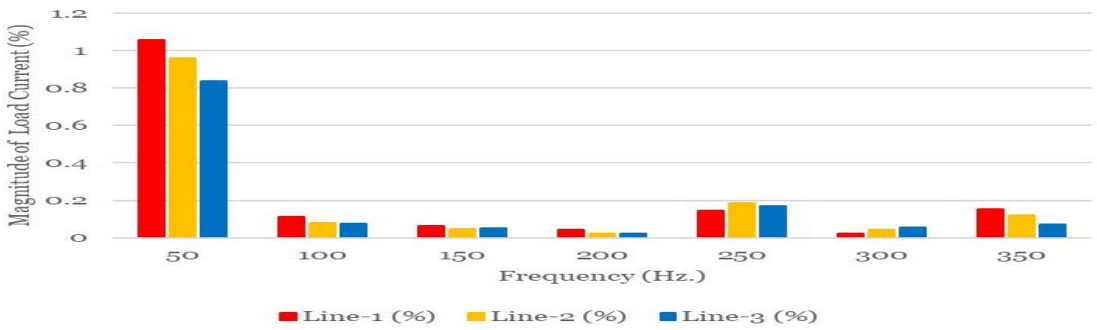

Fig. 26 Magnitude of load current (%) versus frequency

Table 6. Comparison of % THD of source and load current with LCL compensation

		Source current (%)	Load current (%)
S.no.	Electrical Quantity	Percentage (%)	Percentage (%)
1.	% THD of I_{L1}	0.085	23.89
2.	% THD of I_{L2}	0.099	25.61
3.	% THD of I_{L3}	0.103	25.49

4.CONCLUSION

Firstly, shunt APFs without LCL filters rely on simpler L-type output filters, which are less effective at suppressing high-frequency switching harmonics. This increases total harmonic distortion (THD) in grid currents. Secondly, L-series filters require larger inductors to achieve comparable attenuation, leading to heavier, costlier designs with practical sizing challenges. Thirdly, capacitive loads amplify harmonic currents due to their frequency-dependent impedance, destabilizing the system. Conventional models often fail to account for this, risking instability.

Table 7. % THD comparison of source, filter and load side current

,

Case.	Method	Term	$\%I_s$	With solar $\%I_L$
1	Without Filter and LCL compensation	%THD Line-1	23.65	23.65
		%THD Line-2	36.45	36.35
		%THD Line-3	39.42	39.42
2	PWM without LCL Compensation	%THD Line-1	0.601	20.36
		%THD Line-2	0.451	30.65
		%THD Line-3	0.296	33.96
3	PWM with LCL Compensation	%THD Line-1	0.085	23.89
		%THD Line-2	0.099	25.61
		%THD Line-3	0.103	25.49

LCL filters add capacitors and inductors, raising costs and design complexity. Hence, passive damping resistors also increase power losses. Overall LCL compensation enhances harmonic filtering but demands sophisticated control and careful damping design. Since systems without LCL filters face inherent limitations in attenuation and load adaptability, often necessitating larger components. AC while eliminating source-side current distortions. The novel PWM validated through comparative analysis of source and load currents under varying compensation configurations. The key innovations include the LCL compensation network by slightly increasing source resistance at the grid side by filtering high-frequency switching notches. The SAPF's synchronization with grid voltage via advanced phase-locked loops (PLLs) enhances harmonic detection accuracy, enabling real-time adaptation to grid disturbances. The system integrates a Perturbed and Observed (P&O) algorithm to optimize power extraction from the solar PV array. By correlating voltage sensor data with PWM switching signals, the controller dynamically adjusts power flow to mitigate voltage fluctuations caused by load shifts or solar variability. This work bridges critical gaps in renewable energy integration, offering a scalable solution for harmonizing solar generation with grid stability.

REFERENCES

[1] Kumar GB, Palanisamy K, Sanjeevikumar P, Muyeen SM., "Analysis of control strategies for smoothing of solar PV fluctuations with storage devices", Energy Reports, 2023 Dec 1; 9:163-77, doi:10.1016/j.egyr.2022.11.176

[2] Y. Wang, O. Lucia, Z. Zhang, S. Gao, Y. Guan and D. Xu, "A Review of High Frequency Power Converters and Related Technologies," in IEEE Open Journal of the Industrial Electronics Society, vol. 1, pp. 247-260, 2020, doi: 10.1109/OJIES.2020.3023691

[3] J. Ye et al., "An Accurate Dead Time Compensation Method for SPWM Voltage Source Inverters", in IEEE Transactions on Power Electronics, vol. 38, no. 4, pp. 4894-4908, April 2023, doi: 10.1109/TPEL.2022.3226865

[4]Milasi, R.M., Lynch, A.F., Li, Y. Adaptive control of an active power filter for harmonic suppression and power factor correction. Int. J. Dynam. Control 10, 473–482 (2022), doi:10.1007/s40435-25-0

[5] Khan M.Z., Agrawal S., "Economic Control of Solar Photo-Voltaic Generation System using Efficient Scheme of Novel One Cycle Modulator for Direct Current Supply", Renewable Energy Research and Applications (2024) 5(1) 63-72, doi: 10.22044/rera.2023.12715.1202

[6]] Krishnakumar, V., Anbarasan, P., Venmathi, M., Pradeep, J. (2024). Recent challenges and reviews on sensorless, PWM techniques and controller possibilities of permanent magnet motors for electric vehicle applications. International Journal of Ambient Energy, 45(1), doi: 10.1080/01430750.2023.2281613

[7] Y. Wang, X. Wu, Y. Hou, P. Cheng, Y. Liang and L. Li, "Full-Range LED Dimming Driver with Ultrahigh Frequency PWM Shunt Dimming Control", in IEEE Access, vol. 8, pp. 79695-79707, 2020, doi: 10.1109/ACCESS.2020.2990400

[8] M. Iqbal et al., "Neural Networks Based Shunt Hybrid Active Power Filter for Harmonic Elimination," in IEEE Access, vol. 9, pp. 69913-69925, 2021, doi: 10.1109/ACCESS.2021.3077065

[9] B. A. Martínez-Treviño, A. E. Aroudi, H. Valderrama-Blavi, A. Cid-Pastor, E. Vidal-Idiarte and L. Martinez-Salamero, "PWM Nonlinear Control with Load Power Estimation for Output Voltage Regulation of a Boost Converter with Constant Power Load," in IEEE Transactions on Power Electronics, vol. 36, no. 2, pp. 2143-2153, Feb. 2021, doi: 10.1109/TPEL.2020.3008013

[10] V. P. R K and A. N, "Design and Control of Shunt Active Power Filter for Power Quality Improvements with PV Array," 2024 Third International Conference on Power, Control and Computing Technologies (ICPC2T), Raipur, India, 2024, pp. 55-59, doi: 10.1109/icpc2t60072.2024.10475117

[11] Khan, Mohammed Zaid, Surender Singh Tanwar, Ravindra Dayama, Rahul Raj Choudhary, Ravindra Mangal. "Conversion of Impulse Voltage Generator into Steep Wave Impulse Test-Equipment." In International Journal of Modern Physics: Conference Series, vol. 22, pp. 637-644. World Scientific Publishing Company 2013, doi:10.1142/S2010194513010787

[12] A.K. Paul, Sai Ram B., S.V. Kulkarni, Review of coupled inductors in power electronics: From concept to practice, e-Prime - Advances in Electrical Engineering, Electronics and Energy, volume 8,2024,100501, ISSN 2772 6711, doi:10.1016/j.prime.2024.100501

[13] Sun T, Sun Y, Ma B, Bu F, Qin Y, Liu Q, Deaconu SI. A comprehensive review on the comparison and performance of five-phase space vector pulse width modulation overmodulation strategies. Energies. 2024; 17(6):1356, doi: 10.3390/en17061356

[14] J. Ye et al., "An Accurate Dead Time Compensation Method for SPWM Voltage Source Inverters," in IEEE Transactions on Power Electronics, vol. 38, no. 4, pp. 4894-4908, April 2023, doi: 10.1109/TPEL.2022.3226865

[15] S. A. Saleh, "Development and Performance Testing of a V/f Control for Permanent Magnet Synchronous Motor Drives with Wavelet Modulated Power Electronic Converters," in IEEE Transactions on Industry Applications, doi: 10.1109/TIA.2024.3362917

[16] Husain et al., "Electric Drive Technology Trends, Challenges, and Opportunities for Future Electric Vehicles," in Proceedings of the IEEE, vol. 109, no. 6, pp. 1039-1059, June 2021, doi: 10.1109/JPROC.2020.3046112

[17] H. Borland, "Optimised MV neutral treatment and earth fault management," 2022 IEEE/PES Transmission and Distribution Conference and Exposition (T&D), New Orleans, LA, USA, 2022, pp. 1-5, doi: 10.1109/TD43745.2022.9816980

[18] H. Tian, W. Han, M. Chen, G. Liang and Z. Tang, "Common-Ground-Type Inverter with Dynamic Boosting and Compensation for Grid," in IEEE Transactions on Power Electronics, vol. 39, no. 5, pp. 6017-6027, May 2024, doi: 10.1109/TPEL.2024.3368559

[19] Ostapchuk O, Kuznetsov V, Kruczek W, Kuznetsov V, Tsyplenkov D., "Analysis of the neutral grounding modes influence on the reliability characteristics of local systems with renewable energy sources," Diagnostyka. 2021;22, doi:10.29354/DIAG/132834

[20] W. Xu, W. Zhu and Z. Shu, "Suppression of DC Voltage Ripple Impact on Non-Isolated Single-Phase Half-Bridge Unified Power Quality Conditioner," in IEEE Transactions on Industrial Electronics, doi: 10.1109/tie.2023.3337497

[21] Khan S, Rahman K, Tariq M, Hameed S, Alamri B, Babu TS. Solid-State Transformers: Fundamentals, Topologies, Applications, and Future Challenges. Sustainability. 2022; 14(1):319, doi: 10.3390/su14010319

[22] M. Z. Khan and S. Agrawal, "Enhancement of Improving Power Quality Using Solar PV Novel Shunt Active Power Filter and Advanced MPPT Algorithms," 2025 Fifth International Conference on Advances in Electrical, Computing, Communication and Sustainable Technologies (ICAECT), Bhilai, India, 2025, pp. 1-6, doi: 10.1109/ICAECT63952.2025.10958896